# Optomechanically-induced-transparency cooling of massive mechanical resonators to the quantum ground state

Yong-Chun Liu and Yun-Feng Xiao\*

State Key Laboratory for Mesoscopic Physics and School of Physics, Peking University; Collaborative Innovation Center of Quantum Matter, Beijing 100871, P. R. China

Xingsheng Luan and Chee Wei Wong<sup>†</sup>

Optical Nanostructures Laboratory, Columbia University, New York, NY 10027, USA (Dated: August 29, 2018)

Ground state cooling of massive mechanical objects remains a difficult task restricted by the unresolved mechanical sidebands. We propose an optomechanically-induced-transparency cooling scheme to achieve ground state cooling of mechanical motion without the resolved sideband condition in a pure optomechanical system with two mechanical modes coupled to the same optical cavity mode. We show that ground state cooling is achievable for sideband resolution  $\omega_{\rm m}/\kappa$  as low as  $\sim 0.003$ . This provides a new route for quantum manipulation of massive macroscopic devices and high-precision measurements.

PACS numbers: 42.50.Wk, 07.10.Cm, 42.50.Lc Key words: ground state cooling, resolved sideband limit, optomechanics

#### INTRODUCTION

Cavity optomechanics provides a perfect platform not only for the fundamental study of quantum theory but also for the broad applications in quantum information processing and high-precision metrology [1–3]. For most applications it is highly desirable to cool the mechanical motion to the quantum ground state by suppressing thermal noise. In the past few years numerous efforts have made strides towards this goal through backaction cooling [4–13]. However, the cooling limit is subjected to quantum backaction, and ground state cooling is possible only in the resolved sideband (good-cavity) limit [14, 15], which requires the resonance frequency of the mechanical motion  $(\omega_m)$  to be larger than the cavity decay rate  $\kappa$ . This sets a major obstacle for the ground state preparation and quantum manipulation of macroscopic and mesoscopic mechanical resonators with typically low mechanical resonance frequency. Therefore, it is essential to overcome this limitation, so that ground state cooling can be achieved irrespective of mechanical resonance frequency and cavity damping.

Some recent proposals [16] focus on circumventing the resolved sideband restriction by using dissipative coupling mechanism [17, 18], parameter modulations [19-23] and hybrid systems [24-29]. Here we propose a unresolvedsideband ground-state cooling scheme in a generic optomechanical system which does not require modified mechanisms of coupling or specific modulation of the system parameters, or additional components. We take advantage of the destructive quantum interference in a cavity optomechanical system with two mechanical modes coupled to the same optical cavity mode, where optomechanically-induced transparency (OMIT) phenomenon [30–33] occurs. We show that with the help of quantum interference, ground state cooling of the mechanical mode with  $\omega_{\rm m} \ll \kappa$  can be achieved. Moreover, we examine the multiple input cascaded OMIT cooling which further suppresses the quantum backaction heating. This ren-

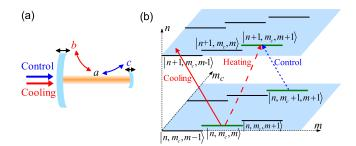


FIG. 1: (color online) (a) Sketch of a typical optomechanical system with two mechanical modes b and c coupled to the same optical cavity mode a. The cavity is driven by a cooling laser and a control laser. (b) Energy level diagram of the system.  $|n,m_c,m\rangle$  denotes the state of n photons,  $m_c$  c-mode phonons and m b-mode phonons in the displaced frame. The red solid (dashed) arrow denotes the cooling (heating) process of mode b. The blue dotted arrow denotes the control laser enhanced coupling between mechanical mode c and the optical cavity mode a.

ders quantum optomechanics with low optical-Q cavities and low mechanical frequency resonators.

### MODEL

In a generic optomechanical system, as shown in Fig. 1(a), we consider an optical cavity mode a coupled to two mechanical resonance modes b and c, where b is the mode to be cooled and c is a control mode. The cavity is driven by a cooling laser and a control laser, with frequencies  $\omega_0$  and  $\omega_1$ , respectively. In the frame rotating at the cavity resonance frequency  $\omega_c$ , the system Hamiltonian reads as

$$H = H_b + H_c,$$

$$H_b = \omega_{\rm m} b^{\dagger} b + g a^{\dagger} a (b + b^{\dagger}) + (\Omega_0^* a e^{i \Delta_0 t} + \text{H.c.}),$$

$$H_c = \omega_{\rm mc} c^{\dagger} c + g_c a^{\dagger} a (c + c^{\dagger}) + (\Omega_1^* a e^{i \Delta_1 t} + \text{H.c.}). \quad (1)$$

Here  $H_b$  ( $H_c$ ) describes the Hamiltonian related with mode b (c);  $\omega_{\rm m}$  ( $\omega_{\rm mc}$ ) is the resonance frequency of mode b (c); g and  $g_c$  denote the single-photon optomechanical coupling rates;  $\Omega_0$  ( $\Omega_1$ ) represents the driving strength and  $\Delta_0 = \omega_0 - \omega_c$  ( $\Delta_1 = \omega_1 - \omega_c$ ) is the frequency detuning between the cooling (control) laser and the cavity mode. For strong driving, the linearized system Hamiltonian is given by

$$H_L = \omega_{\rm m} b_1^{\dagger} b_1 + [G^{(t)} a_1^{\dagger} + G^{(t)*} a_1] (b_1 + b_1^{\dagger}) + \omega_{\rm mc} c_1^{\dagger} c_1 + [G_c^{(t)} a_1^{\dagger} + G_c^{(t)*} a_1] (c_1 + c_1^{\dagger}).$$
 (2)

Here the operators  $a_1, b_1$  and  $c_1$  describe the quantum fluctuations around the corresponding classical mean fields after the linearization;  $G^{(t)} = g(\alpha_0 e^{-i\Delta_0't} + \alpha_1 e^{-i\Delta_1't})$  and  $G_{\rm c}^{(t)} = g_{\rm c}(\alpha_0 e^{-i\Delta_0't} + \alpha_1 e^{-i\Delta_1't})$  are the light-enhanced optomechanical coupling strengths, with modified detunings  $\Delta_0' = \Delta_0 + \Delta_{\rm om}, \Delta_1' = \Delta_1 + \Delta_{\rm om}$  and  $\Delta_{\rm om} = 2(g^2/\omega_{\rm m} + g_{\rm c}^2/\omega_{\rm mc})(|\alpha_0|^2 + |\alpha_1|^2)$ ;  $\alpha_0$  and  $\alpha_1$  are the intracavity field from the contribution of the cooling and control laser inputs;  $\kappa, \gamma (\equiv \omega_{\rm m}/Q_{\rm m})$  and  $\gamma_{\rm c} (\equiv \omega_{\rm mc}/Q_{\rm mc})$  are the energy decay rates of the modes a, b and c.

## QUANTUM NOISE SPECTRUM

The optical force acting on mode b takes the form  $F=-[G^{(t)*}a_1+G^{(t)}a_1^{\dagger}]/x_{\rm ZPF}$ , where  $x_{\rm ZPF}$  is the zero-point fluctuation. The quantum noise spectrum of the optical force  $S_{FF}(\omega)\equiv\int dt e^{i\omega t} \left\langle F(t)F(0) \right\rangle$  is calculated to be

$$S_{FF}(\omega) = \sum_{j=0}^{1} S_{FF}^{j}(\omega),$$

$$S_{FF}^{j}(\omega) = \frac{g^{2}}{x_{\text{ZPF}}^{2}} |\alpha_{j} \tilde{\chi}_{j}(\omega)|^{2}$$

$$\times \left[\kappa + g_{c}^{2} \sum_{k=0}^{1} |\alpha_{k}|^{2} \tilde{\chi}_{\text{mc}} \left(\omega + \Delta_{j}^{\prime} - \Delta_{k}^{\prime}\right)\right], (3)$$

where  $\tilde{\chi}_j^{-1}(\omega) = \chi_j^{-1}(\omega) + g_{\rm c}^2 \sum_{k=0}^1 |\alpha_k|^2 \left[\chi_{\rm mc}(\omega + \Delta_j' - \Delta_k') + \chi_{\rm mc}^*(-\omega - \Delta_j' + \Delta_k')\right], \ \tilde{\chi}_{\rm mc}(\omega) = \gamma_{\rm c}(n_{\rm c,th} + 1)|\chi_{\rm mc}(\omega)|^2 + \gamma_{\rm c}n_{\rm c,th}|\chi_{\rm mc}(-\omega)|^2, \ \chi_j^{-1}(\omega) = -i(\omega + \Delta_j') + \kappa/2 \ {\rm and} \ \chi_{\rm mc}^{-1}(\omega) = -i(\omega - \omega_{\rm mc}) + \gamma_{\rm c}/2, \ {\rm with} \ {\rm integers} \ j \ {\rm and} \ k \ {\rm being} \ {\rm the} \ {\rm summation} \ {\rm indices}. \ {\rm Here} \ \chi_j(\omega) \ {\rm represent} \ {\rm the} \ {\rm optical} \ {\rm response} \ {\rm to} \ {\rm the} \ {\rm input} \ {\rm light} \ {\rm and} \ \chi_{\rm mc}(\omega) \ {\rm is} \ {\rm the} \ {\rm response} \ {\rm function} \ {\rm of} \ {\rm the} \ {\rm control} \ {\rm mechanical} \ {\rm mode}; \ n_{\rm th} = 1/[e^{\hbar\omega_{\rm mc}/(k_{\rm B}T)} - 1] \ {\rm and} \ n_{\rm c,th} = 1/[e^{\hbar\omega_{\rm mc}/(k_{\rm B}T)} - 1] \ {\rm are} \ {\rm the} \ {\rm thermal} \ {\rm phonon} \ {\rm numbers} \ {\rm of} \ {\rm modes} \ b \ {\rm and} \ c \ {\rm at} \ {\rm the} \ {\rm environmental} \ {\rm temperature} \ T.$ 

In conventional single mechanical mode approach, the quantum noise spectrum exhibits a standard Lorentzian curve [15]. However, here due to the interaction between the control mechanical and the optical cavity modes, the noise spectrum [Eq. (3)] is modified to a non-Lorentzian lineshape. This originates from the quantum interference manifested by OMIT. As shown in Fig. 1(b), the system here contains a series of three-level subsystems relevant with OMIT for heating suppression. In the presence of the control field, the transition amplitude

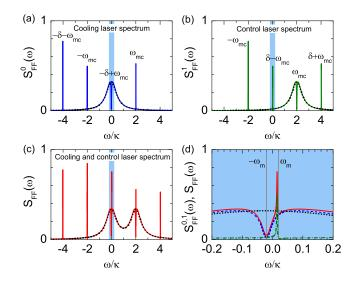


FIG. 2: (color online) Quantum noise spectra (arbitrary units). The solid curves denote (a)  $S_{FF}^0(\omega)$ , (b)  $S_{FF}^1(\omega)$  and (c)  $S_{FF}(\omega)$  for  $\omega_{\rm m}/\kappa=0.02, \omega_{\rm mc}/\kappa=2, \Delta_0'=\omega_{\rm m}, \Delta_1'=-\omega_{\rm mc}, g/\omega_{\rm m}=10^{-3}, g_c/\omega_{\rm mc}=5\times10^{-4}, \alpha_0=\alpha_1=10^3, Q_{\rm mc}=10^4$  and  $n_{\rm th}=10^3$ . The black dotted curves in (a)-(c) correspond to the results without the control mode ( $g_c=0$ ). In (a) and (b), the position of the sharp peaks and dips are marked. (d) Zoom-in view of the shaded region in (a)-(c).  $S_{FF}^0(\omega)$ , blue dashed curve;  $S_{FF}^1(\omega)$ , green dashed-dotted curve;  $S_{FF}(\omega)$ , red solid curve. The black dotted curves corresponds to the result without the control mode and the control laser  $[S_{FF}^{0,0}(\omega)]$ . The gray vertical lines denote  $\omega=\pm\omega_{\rm m}$ .

between the two pathways (red dashed arrow and blue dotted arrow) destructively interfere, leading to the suppression of the heating transition.

For the unresolved sideband regime ( $\omega_{\rm m} \ll \kappa$ ), the quantum noise spectra are plotted in Fig. 2 with parameters  $Q_{\rm mc}=10^4$  and  $n_{\rm th}=10^3$ . Note that  $S_{FF}^0(\omega)$  corresponds to the spectrum associated with the cooling laser (with detuning  $\Delta'_0$ ) and  $S^1_{FF}(\omega)$  represents the spectrum related to the control laser (with detuning  $\Delta'_1$ ). Without the control mechanical mode  $(g_{\rm c}=0)$ , they reduce to  $S_{FF}^{0,0}(\omega)=\kappa\left|\alpha_0\chi_0\left(\omega\right)\right|^2g^2/x_{\rm ZPF}^2$  and  $S_{FF}^{1,0}(\omega)=$  $\kappa \left| \alpha_1 \chi_1 \left( \omega \right) \right|^2 g^2 / x_{\mathrm{ZPF}}^2$  , which are Lorentzians with the centers at  $\omega = -\Delta_0'$  and  $-\Delta_1'$  [black dotted curves in Figs. 2(a) and 2(b)], respectively. In contrast, with the presence of the control mode, a series of OMIT resonances appear in the spectra. For  $S_{FF}^0(\omega)$ , those dips/peaks are located at  $\omega = \pm \omega_{\rm mc}$ ,  $-\delta \pm \omega_{\rm mc}$  [Fig. 2(a)], where  $\delta \equiv \Delta_0' - \Delta_1'$  represents the twophoton detuning of the input lasers. Thereinto, the resonances at  $\omega = \pm \omega_{\rm mc}$  originate from the interaction between the cooling laser and mode c, which changes the mode density for the cavity field to absorb/emit a phonon with energy  $\hbar\omega_{\rm mc}$ ; the resonances at  $\omega = -\delta \pm \omega_{\rm mc}$  stem from the interaction among the cooling laser, the control laser and mode c. Analogously, for  $S_{FF}^1(\omega)$ , the resonances are located at  $\omega = \pm \omega_{\rm mc}$ ,  $\delta \pm \omega_{\rm mc}$  [Fig. 2(b)]. For cooling of mode b, the dips/peaks

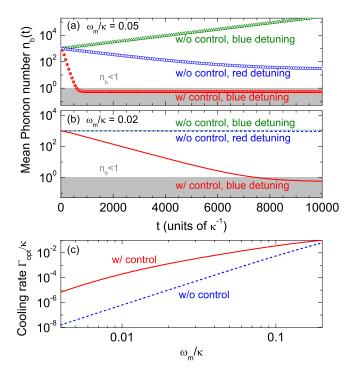


FIG. 3: (color online) (a) Time evolution of the mean phonon number  $n_b(t)$  with control mode (red closed circle) for  $\omega_{\rm m}/\kappa=0.05$ ,  $\omega_{\rm mc}/\kappa=2$ ,  $\Delta_0'=\omega_{\rm m}$ ,  $\Delta_1'=-\omega_{\rm mc}$ ,  $g/\omega_{\rm m}=10^{-3}$ ,  $g_c/\omega_{\rm mc}=5\times10^{-4}$ ,  $\alpha_0=1200$ ,  $\alpha_1=1600$ ,  $Q_{\rm mc}=10^4$ ,  $Q_{\rm m}=10^5$  and  $n_{\rm th}=10^3$ . The results without the control mode and the control laser ( $g_c=0$ ,  $\alpha_1=0$ ) for  $\Delta_0'=-\omega_{\rm m}$  (blue open circle) and  $\Delta_0'=\omega_{\rm m}$  (green triangles) are plotted for comparison. (b) Same as (a) except that  $\omega_{\rm m}/\kappa=0.02$  and  $\alpha_0=\alpha_1=10^3$ . The shaded regions in (a) and (b) denote  $n_b<1$ . (c) Cooling rates  $\Gamma_{\rm opt}$  as functions of  $\omega_{\rm m}$  in the unit of  $\kappa$  with the presence (red solid curve) and absence (blue dashed curve) of the control mode and the control laser; the parameters are the same as Fig. 3(b).

at  $\omega=\pm\omega_{\rm m}$  are relevant, since  $A_{\mp}\equiv S_{FF}\left(\pm\omega_{\rm m}\right)x_{\rm ZPF}^2$  are the rates for absorbing and emitting a b-mode phonon by the cavity field, corresponding to the cooling and heating of mode b, respectively. With the appropriate value of the two-photon detuning at  $\delta=\omega_{\rm mc}+\omega_{\rm m}$ , the OMIT lineshapes in  $S_{FF}(\omega)$  can be tuned to appear at  $\omega=\pm\omega_{\rm m}$ , as shown in Figs. 2(c) and 2(d). At  $\omega=-\omega_{\rm m}$ , it exhibits a deep OMIT window, which reveals the suppression of heating process, originating from the destructive interference. Although a shallow dip also appears at  $\omega=\omega_{\rm m}$ , it only slightly decreases the mode density. The reason the center ( $\omega=-\Delta_1'$ ) of the Lorentzian background in  $S_{FF}^{1,0}(\omega)$ , as shown in Fig. 2(b).

#### COVARIANCE APPROACH

To verify the destructive quantum interference effect, we next solve the quantum master equation and use covariance approach [34, 35] to obtain exact numerical results. The master equation is given by  $\dot{\rho}=i[\rho,H_L]+\kappa\mathcal{D}[a_1]\rho+\gamma(n_{\rm th}+m_{\rm th})$ 

1) $\mathcal{D}[b_1]\rho + \gamma n_{\rm th} \mathcal{D}[b_1^{\dagger}]\rho + \gamma_{\rm c}(n_{\rm c,th} + 1)\mathcal{D}[c_1]\rho + \gamma_{\rm c}n_{\rm c,th} \mathcal{D}[c_1^{\dagger}]\rho$ , where  $\mathcal{D}[\hat{o}]\rho = \hat{o}\rho\hat{o}^{\dagger} - (\hat{o}^{\dagger}\hat{o}\rho + \rho\hat{o}^{\dagger}\hat{o})/2$  denotes the the standard dissipator in Lindblad form. In Fig. 3(a) and 3(b) we plot the time evolution of the mean phonon number  $n_b(t)$  for typical parameters. For single mechanical mode case in the unresolved sideband regime, with red detuning input laser, the mechanical motion is only slowly cooled with a small cooling rate (net optical damping rate)  $\Gamma_{\rm opt} \equiv A_- - A_+$ , without reaching the ground state. However, in the presence of the control mode and the control laser, the cooling rate can be enhanced for more than two orders of magnitude [Fig. 3(c)], and ground state cooling with mean phonon number  $n_b < 1$ is achievable, even for sideband resolution  $\omega_{\rm m}/\kappa$  as small as 0.02. It should be emphasized that in this case the cooling laser is blue detuned, which is quite different from the single mechanical mode approach. For the latter, blue detuning leads to amplification instead of cooling of the mechanical motion. The blue-detuning cooling is the unique property originating from the quantum interference which modifies the noise spectrum of the optical force. The OMIT lineshape can be viewed as the inverse of the standard Lorentzian, thus the detunings for cooling are just opposite to that for the single mechanical mode case.

#### CASCADED OMIT COOLING

To further suppress quantum backaction heating, we propose the use of additional coherent laser inputs, resulting in cascaded OMIT cooling. For N inputs, the quantum noise spectrum of the optical force takes the same form as Eq. (3) except that the summation indices (j, k) run from 0 to N - 1. As displayed in Figs. 4(a)-4(d), for two inputs, the suppression of heating for mode b is the contribution of suppressed  $A_+^0 \equiv S_{FF}^0(-\omega_{\rm m}) x_{\rm ZPF}^2$ , while  $A_-^1 \equiv S_{FF}^1(\omega_{\rm m}) x_{\rm ZPF}^2$  is also slightly suppressed. In the presence of the third input laser with detuning  $\Delta_2' = \Delta_0' - 2(\omega_{\rm mc} + \omega_{\rm m})$ , the interaction involved with the control mode results in the suppression of  $A_+^1 \equiv S_{FF}^1(-\omega_{\rm m})x_{\rm ZPF}^2$  and  $A_-^2 \equiv S_{FF}^2(\omega_{\rm m})x_{\rm ZPF}^2$ . This results in the net optical damping rate  $\Gamma_{\rm opt} \equiv \sum_{k=0}^{2} (A_{-}^{k} A_+^k$ )  $\simeq A_-^0 - A_+^2$  [Fig. 4(c) and (d)]. More generally, for N inputs with detuning  $\Delta_k' = \Delta_0' - k(\omega_{\rm mc} + \omega_{\rm m})$  (k = 1, 2, ... N - 1), we obtain  $\Gamma_{\rm opt} \simeq A_-^0 - A_+^{N-1}$ . Note that the remaining heating rate  $A_{+}^{N-1}$  is much smaller than the original heating rate due to the large detuning  $\Delta'_k$  for the (N-1)th input. In Fig. 4(e) we compare the cooling dynamics between two inputs and three inputs for typical parameters, which shows that the cascaded OMIT cooling enables larger cooling rate and lower cooling limit, with ground state cooling achievable even for  $\omega_{\rm m}/\kappa = 0.01$ .

#### **COOLING LIMITS**

In Fig. 5 the fundamental cooling limits  $n_{\rm min}$  as functions of the sideband resolution  $\omega_{\rm m}/\kappa$  are plotted. The exact

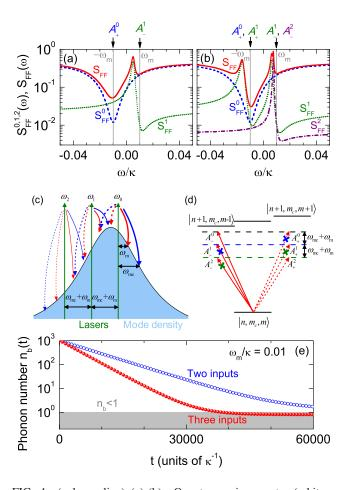


FIG. 4: (color online) (a)-(b): Quantum noise spectra (arbitrary units) for two inputs (a) and three inputs (b).  $S_{FF}(\omega)$ , red solid curve;  $S_{FF}^0(\omega)$ , blue dashed curve;  $S_{FF}^1(\omega)$ , green dotted curve;  $S_{FF}^2(\omega)$ , purple dashed-dotted curve. The gray vertical lines denote  $\omega=\pm\omega_{\rm m}$ . (c) Scattering interpretation of optomechanical interactions with three inputs. The shaded Lorentzian represents the mode density of the optical cavity. The green vertical arrows denote the input lasers. The solid (dashed) curved arrows denote the anti-Stokes (Stokes) scattering processes relevant with mode b (red) and mode c (blue). (d) Energy levels and interpretation of the suppression (denoted by the "×") of heating and cooling with three inputs. (e) Time evolution of the mean phonon number  $n_b(t)$  with two inputs (blue open circle) and three inputs (red closed circle). The shaded region denotes  $n_b < 1$ . Here  $\alpha_2 = 10^3$ ,  $\omega_{\rm mc}/\kappa = 2$ ,  $\omega_{\rm m}/\kappa = 0.01$  and other parameters are the same as Fig. 3 (b).

numerical results are obtained from master equation simulations. The black dotted curve shows the best result for conventional single mechanical mode approach, given by  $n_{\rm min}=\kappa/(4\omega_{\rm m})$ , which is obtained when  $\Delta_0'=-\kappa/2$  [14]. It reveals the great advantage of OMIT cooling and cascaded OMIT cooling, with possibility for ground state cooling even when  $\omega_{\rm m}/\kappa\sim3\times10^{-3}$ , which goes beyond the resolved sideband limit by nearly 3 orders of magnitude. Note that Fig. 5 shows the cooling limits increase as  $\omega_{\rm m}/\kappa$  increases from  $\sim0.02$  to a larger value. This is a result of blue detuning induced heating, which becomes significant when  $\omega_{\rm m}/\kappa$  is large.

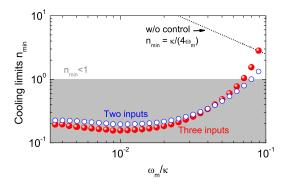


FIG. 5: (color online) Fundamental cooling limits  $n_{\rm min}$  as functions of  $\omega_{\rm m}/\kappa$  for two inputs (red closed circles) and three inputs (blue open circles). The result for single mechanical mode approach (black dotted curve) is plotted for comparison. The shaded region denotes  $n_{\rm min} < 1$ . Here  $\alpha_0 = \alpha_1 = \alpha_2 = 500$  and other parameters are the same as Fig. 4.

#### EXPERIMENTAL FEASIBILITY

It should be stressed that the OMIT cooling described here adds little complexity to the existing optomechanical system, which is crucial in the experimental point of view. Compared with the conventional backaction cooling approach, the additional requirement here is a control mechanical mode and one (or more) input laser. It is experimentally feasible for various optomechanical systems within current technical conditions. On one hand, many optomechanical systems possess abundant mechanical modes with different resonance frequencies, since the oscillation have different types and orders. This situation can be found in optomechanical systems using whispering-gallery microcavities [36, 37], photonic crystal cavities [38, 39], membranes [40, 41], nanostrings [42] and nanorods [43, 44] amongst others. Usually only one mechanical mode is used in most optomechanical experiments, while exciting an additional mechanical mode is often unintended. On the other hand, composite optomechanical systems, containing two independent mechanical resonators, are also conceivable. For example, in Fabry-Pérot cavities, the motion of one mirror acts as an control mechanical mode while the other mirror is to be cooled [Fig. 1(a)]. In the near-field optomechanical system [42], to cool the nanostrings, the control mode can be selected from the vibration of the microtoroid.

# CONCLUSION

In summary, we have presented the OMIT cooling scheme allowing ground state cooling of mechanical resonators beyond the resolved sideband limit. It is demonstrated that by employing the OMIT interference, quantum backaction heating can be largely suppressed, extending the fundamental limit of backaction cooling. The scheme is experimentally feasible, which requires another control mechanical mode and multiple laser inputs. Such a M-O-M system (M, mechanical mode; O,

optical mode) studied here offers potential for cooling enormous mass scale resonators [45, 46], which possess small resonance frequencies. Together with the recently examined multi-optical-mode [28, 47–50] and multi-mechanical-mode [51–55] systems,it is shown that such interference effect in multi-mode cavity optomechanics provides unique advantage for both fundamental studies and broad applications. Recently we noticed a related work [56], but here we use the covariance approach to examine the fundamental cooling limits and present detailed analysis of cascaded OMIT cooling. This paves the way for the manipulation of macroscopic mechanical resonators in the quantum regime.

Y.-C.L. and Y.-F.X were supported by the National Basic Research Program of China (No. 2013CB328704, No. 2013CB921904), National Natural Science Foundation of China (Nos. 11474011, 11222440, and 61435001), and Research Fund for the Doctoral Program of Higher Education of China (No. 20120001110068). X.L. and C.W.W were supported by the Optical Radiation Cooling and Heating in Integrated Devices program of Defense Advanced Research Projects Agency (contract number C11L10831).

- \* Electronic address: yfxiao@pku.edu.cn; URL: www.phy.pku.edu.cn/~yfxiao/index.html
- † Electronic address: cww2014@columbia.edu
- [1] Kippenberg T J, Vahala K J. Cavity optomechanics: Backaction at the mesoscale. Science, 2008, 321: 1172
- [2] Aspelmeyer M, Kippenberg T J, Marquardt F. Cavity optomechanics. arXiv:1303.0733, 2013
- [3] Meystre P. A short walk through quantum optomechanics. Ann Phys, 2013, 525: 215
- [4] Teufel J D, Donner T, Li D, Harlow J W, Allman M S, Cicak K, Sirois A J, Whittaker J D, Lehnert K W, Simmonds R W. Sideband cooling of micromechanical motion to the quantum ground state. Nature (London), 2011, 475: 359
- [5] Chan J, Mayer Alegre T P, Safavi-Naeini A H, Hill J T, Krause A, Gröblacher S, Aspelmeyer M, Painter O. Laser cooling of a nanomechanical oscillator into its quantum ground state. Nature (London), 2011, 478: 89
- [6] Gigan S, Böhm H R, Paternostro M, Blaser F, Langer G, Hertzberg J B, Schwab K C, Bäuerle D, Aspelmeyer M, Zeilinger A. Self-cooling of a micromirror by radiation pressure. Nature (London), 2006, 444: 67
- [7] Arcizet O, Cohadon P F, Briant T, Pinard M, Heidmann A. Radiation-pressure cooling and micromechanical instability of a micromirror. Nature (London), 2006, 444: 71
- [8] Schliesser A, Del'Haye P, Nooshi N, Vahala K J, Kippenberg T J. Radiation pressure cooling of a micromechanical oscillator using dynamical backaction. Phys Rev Lett, 2006, 97: 243905
- [9] Schliesser A, Rivière R, Anetsberger G, Arcizet O, Kippenberg T J. Resolved-sideband cooling of a micromechanical oscillator. Nature Phys, 2008, 4: 415
- [10] Gröblacher S, Hertzberg J B, Vanner M R, Cole G D, Gigan S, Schwab K C, Aspelmeyer M. Demonstration of an ultracold micro-optomechanical oscillator in a cryogenic cavity. Nature Phys, 2009, 5: 485
- [11] Park Y S, Wang H. Resolved-sideband and cryogenic cooling

- of an optomechanical resonator. Nature Phys, 2009, 5: 489
- [12] Schliesser A, Arcizet O, Rivère R, Anetsberger G, Kippenberg T J. Resolved-sideband cooling and position measurement of a micromechanical oscillator close to the Heisenberg uncertainty limit. Nature Phys, 2009, 5: 509
- [13] Rocheleau T, Ndukum T, Macklin C, Hertzberg J B, Clerk A A, Schwab K C. Preparation and detection of a mechanical resonator near the ground state of motion. Nature (London), 2010, 463: 72
- [14] Wilson-Rae I, Nooshi N, Zwerger W, Kippenberg T J. Theory of ground state cooling of a mechanical oscillator using dynamical backaction. Phys Rev Lett, 2007, 99: 093901
- [15] Marquardt F, Chen J P, Clerk A A, Girvin S M. Quantum theory of cavity-assisted sideband cooling of mechanical motion. Phys Rev Lett, 2007, 99: 093902
- [16] Liu Y C, Hu Y W, Wong C W, Xiao Y F. Review of cavity optomechanical cooling. Chin Phys B, 2013, 22: 114213
- [17] Elste F, Girvin S M, Clerk A A. Quantum noise interference and backaction cooling in cavity nanomechanics. Phys Rev Lett, 2009, 102: 207209
- [18] Xuereb A, Schnabel R, Hammerer K. Dissipative optomechanics in a Michelson-Sagnac interferometer. Phys Rev Lett, 2011, 107: 213604
- [19] Tian L. Ground state cooling of a nanomechanical resonator via parametric linear coupling. Phys Rev B, 2009, 79: 193407
- [20] Li Y, Wu L A, Wang Z D. Fast ground-state cooling of mechanical resonators with time-dependent optical cavities. Phys Rev A, 2011, 83: 043804
- [21] Liao J Q, Law C K. Cooling of a mirror in cavity optomechanics with a chirped pulse. Phys Rev A, 2011, 84: 053838
- [22] Wang X, Vinjanampathy S, Strauch F W, Jacobs K. Ultraefficient Cooling of Resonators: Beating Sideband Cooling with Quantum Control. Phys Rev Lett, 2011, 107: 177204
- [23] Machnes S, Cerrillo J, Aspelmeyer M, Wieczorek W, Plenio M B, Retzker A. Pulsed Laser Cooling for Cavity Optomechanical Resonators. Phys Rev Lett, 2012, 108: 153601
- [24] Genes C, Ritsch H, Vitali D. Micromechanical oscillator ground-state cooling via resonant intracavity optical gain or absorption. Phys Rev A, 2009, 80: 061803(R)
- [25] Vogell B, Stannigel K, Zoller P, Hammerer K, Rakher M T, Korppi M, Jöckel A, Treutlein P. Cavity-enhanced long-distance coupling of an atomic ensemble to a micromechanical membrane. Phys Rev A, 2013, 87: 023816
- [26] Restrepo J, Ciuti C, Favero I. Single-Polariton Optomechanics. Phys Rev Lett, 2014, 112: 013601
- [27] Gu W J, Li G X. Quantum interference effects on ground-state optomechanical cooling. Phys Rev A, 2013, 87: 025804
- [28] Liu Y C, Xiao Y F, Luan X, Wong C W. Ground state cooling of mechanical motion through coupled cavity interactions in the unresolved sideband regime. CLEO: 2013 (Optical Society of America), p.QM2B.2
- [29] Liu Y C, Xiao Y F, Luan X, Gong Q, Wong C W. Coupled cavities for motional ground state cooling and strong optomechanical coupling. Phys Rev A, 2015, 91: 033818
- [30] Weis S, Rivière R, Deléglise S, Gavartin E, Arcizet O, Schliesser A, Kippenberg T J. Optomechanically induced transparency. Science, 2010, 330: 1520
- [31] Safavi-Naeini A H, Alegre T P M, Chan J, Eichenfield M, Winger M, Lin Q, Hill J T, Chang D E, Painter O. Electromagnetically induced transparency and slow light with optomechanics. Nature (London), 2011, 472: 69
- [32] Agarwal G S, Huang S. Electromagnetically induced transparency in mechanical effects of light. Phys Rev A, 2010, 81: 041803(R)

- [33] Qu K, Agarwal G S. Phonon-mediated electromagnetically induced absorption in hybrid opto-electromechanical systems. Phys Rev A, 2013, 87: 031802(R)
- [34] Liu Y C, Xiao Y F, Luan X, Wong C W. Dynamic dissipative cooling of a mechanical resonator in strong coupling optomechanics. Phys Rev Lett, 2013, 110: 153606
- [35] Liu Y C, Shen Y F, Gong Q, Xiao Y F. Optimal limits of cavity optomechanical cooling in the strong coupling regime. Phys Rev A, 2014, 89: 053821
- [36] Kippenberg T J, Rokhsari H, Carmon T, Scherer A, Vahala K J. Analysis of radiation-pressure induced mechanical oscillation of an optical microcavity. Phys Rev Lett, 2005, 95: 033901
- [37] Tomes M, Carmon T. Photonic Micro-Electromechanical Systems Vibrating at X-band (11-GHz) Rates. Phys Rev Lett, 2009, 102: 113601
- [38] Eichenfield M, Chan J, Camacho R M, Vahala K J, Painter O. Optomechanical crystals. Nature (London), 2009, 462: 78
- [39] Zheng J, Li Y, Aras M S, Stein A, Shepard K L, Wong C W. Parametric optomechanical oscillations in two-dimensional slot-type high-Q photonic crystal cavities. App Phys Lett, 2012, 100: 211908
- [40] Thompson J D, Zwickl B M, Jayich A M, Marquardt F, Girvin S M, Harris J G E. Strong dispersive coupling of a high-finesse cavity to a micromechanical membrane. Nature (London), 2008, 452: 72
- [41] Bui C H, Zheng J, Hoch S W, Lee L Y T, Harris J G E, Wong C W. High-reflectivity, high-Q micromechanical membranes via guided resonances for enhanced optomechanical coupling. App Phys Lett, 2012, 100: 021110
- [42] Anetsberger G, Arcizet O, Unterreithmeier Q P, Rivière Q P, Schliesser A, Weig E M, Kotthaus J P, Kippenberg T J. Nearfield cavity optomechanics with nanomechanical oscillators. Nature Phys, 2009, 5: 909
- [43] Zheng J, Sun X, Li Y, Poot M, Dadgar A, Shi N, Pernice W H P, Tang H X, Wong C W. Femtogram dispersive L3-nanobeam optomechanical cavities: design and experimental comparison. Opt Express, 2012, 20: 26484
- [44] Li M, Pernice W H P, Xiong C, Baehr-Jones T, Hochberg M, Tang H X. Harnessing optical forces in integrated photonic cir-

- cuits. Nature (London), 2008, 456: 480
- [45] Abbott B et al. Observation of a kilogram-scale oscillator near its quantum ground state. New J Phys, 2009, 11: 073032
- [46] Abbott B et al. LIGO: The Laser Interferometer Gravitational-Wave Observatory. Rep Prog Phys, 2009, 72: 076901
- [47] Hill J T, Safavi-Naeini A H, Chan J, Painter O. Coherent optical wavelength conversion via cavity-optomechanics. Nature Commun, 2012, 3: 1196
- [48] Dong C, Fiore V, Kuzyk M C, Wang H. Optomechanical dark mode. Science, 2012, 338: 1609
- [49] Liu Y, Davanco M, Aksyuk V, Srinivasan K, Electromagnetically induced transparency and wideband wavelength conversion in silicon nitride microdisk optomechanical resonators. Phys Rev Lett, 2013, 110: 223603
- [50] Bagci T, Simonsen A, Schmid S, Villanueva L G, Zeuthen E, Appel J, Taylor J M, Sørensen A, Usami K, Schliesser A, Polzik E S. Optical detection of radio waves through a nanomechanical transducer. Nature (London), 2014, 507: 81
- [51] Lin Q, Rosenberg J, Chang D, Camacho R, Eichenfield M, Vahala K J, Painter O. Coherent mixing of mechanical excitations in nano-optomechanical structures. Nature Photon, 2010, 4: 236
- [52] Massel F, Cho S U, Pirkkalainen J M, Hakonen P J, Heikkilä P J, Sillanpää M A. Multimode circuit optomechanics near the quantum limit. Nature Commun, 2012, 3: 987
- [53] Seok H, Buchmann L F, Singh S, Meystre P. Optically mediated nonlinear quantum optomechanics. Phys Rev A, 2012, 86: 063829
- [54] Seok H, Buchmann L F, Wright E M, Meystre P. Multimode strong-coupling quantum optomechanics. Phys Rev A, 2013, 88: 063809
- [55] Tan H, Li G, Meystre P. Dissipation-driven two-mode mechanical squeezed states in optomechanical systems. Phys Rev A, 2013, 87: 033829
- [56] Ojanen T, Børkje K. Ground-state cooling of mechanical motion in the unresolved sideband regime by use of optomechanically induced transparency. Phys Rev A, 2014, 90: 013824